

BEAM MEASUREMENTS IN THE HARWELL VARIABLE ENERGY CYCLOTRON

J. D. Lawson

Rutherford High Energy Laboratory, Chilton, Berks., England

Summary

The interpretation of probe measurements of beam behaviour in the cyclotron is discussed with reference to results obtained with the Harwell Variable Energy Cyclotron.

Introduction

A good understanding of orbit dynamics is necessary both for building cyclotrons and for operating them effectively. The emphasis however is different for the two situations; the concepts and formulae of most value to a designer contemplating the construction of a machine are rather different from those of interest to an operator faced with a cyclotron and a set of probes, whose task it is to set it up and extract the beam. Here we review some of the ideas useful in commissioning, and illustrate them with results from the Harwell Variable Energy Cyclotron.

The idea of an equilibrium orbit associated with a particle of specified momentum is well known. Particles displaced from the equilibrium orbit oscillate harmonically about it with vertical and radial frequencies ω_{Q_V} and ω_{Q_R} . Q_R and Q_V are functions of the field modulation (or "flutter"), δ , the gradient of mean field, and their normalized derivatives. In an actual cyclotron the particles pursue spiral orbits, and the equilibrium orbit changes each time a particle crosses the accelerating gap. It is only a useful concept when the change in radius per turn is small. The equilibrium orbit is roughly circular, the departure being a modulation of $(\delta \cos N\theta)/(N^2 - 1)$ where N is the ridge periodicity; this modulation does not affect the general features of the motion, and in what follows it will be ignored (but not forgotten).

In diagnostic work one is confronted with a mixture of effects; in trying to sort them out it is often helpful to have a clear idea of the behaviour of a number of special simple situations, even though these situations are idealized and cannot occur in practice.

Basic Parameters in a "Perfect" Machine

Before discussing actual measurements, we review some familiar basic concepts applicable to isochronous cyclotrons in the energy range already operating, where $\gamma - 1 \ll 1$, so that $\gamma \approx 1 + \frac{1}{2}\beta^2$. β and γ are the usual relativistic parameters, and the normalized energy gain/turn, eV/mc^2 , will be denoted by ϵ . The independent variable describing the motion of a particular particle is taken as θ , the angle swept out since it leaves the source. The principal value of θ is denoted by Θ . Although ϵ is not strictly a continuous

variable, it is approximately true that

$$\frac{1}{2\pi} \int \epsilon d\theta = \gamma - 1 \approx \frac{1}{2} \beta^2 = r^2 \omega^2 / c^2 = r^2 \dot{\theta} \omega^2 \quad (1)$$

To define the particle fully, the amplitude and phase of the radial and vertical oscillations, and the local Q values need to be known as well as Θ or r . An alternative way to characterize the radial oscillations however is in terms of the co-ordinates of the centre of curvature of the orbit (neglecting the flutter modulation). As the particle moves round, the centre of curvature traces out a cusp shaped curve of form shown in fig. 1. A more convenient description when $Q - 1$ is small is in terms of the oscillation amplitude A and the angle ψ , the orientation of the maximum. ψ is defined only once per cycle, but when $Q - 1$ is small, it varies slowly. It is known as the "precession angle", and is given by

$$\psi = \int (1 - Q_R) d\theta \quad (2)$$

In an "ideal" machine with no imperfections a particle in general precesses according to equation 2. Adiabatic damping follows the law $A^2 Q_R \gamma \approx A^2 \gamma^2 = \text{const.}$ and is therefore negligible when $\gamma - 1$ is small.

The motion of a particle through the machine can therefore be described by a set of points on a circle of radius A , each one characterized by a value of ψ and r_1 . Neither ψ nor r_1 is a continuous function of θ , though it is convenient to assume that they are. ψ is undefined by an angle $2\pi(Q - 1)$ and r_1 by an amount ΔR the turn separation. The description we have developed based on the equilibrium orbit concept is not fully adequate therefore for a machine in which the individual turn structure is an important feature. It is however valuable in a machine such as the V.E.C. where such structure is often smeared out.

The beam at any radius can be characterized by a distribution of points on an $A - \psi$ plot, (where ψ is the principal value of ψ) as shown in fig. 1, provided that a suitable convention is introduced to ensure that each particle only appears once. From this we can define the imprecise but useful terms "coherent" and "incoherent" oscillation amplitudes A_c and A_i . (The amplitude written as a vector \vec{A} includes ψ .)

Fig. 1 is not meaningful near the machine centre where the criterion $\gamma - 1 \gg \epsilon$ (or $r \gg \Delta R$) does not apply. The form that it assumes after the first few turns depends in a complicated way on the central geometry. An "open" geometry, as we have in the V.E.C., gives a larger value of A_i than would be the case if defining slits were used. Moving the position of the ion source varies A_c without making much difference to A_i . Normally one tries to adjust A_c to be zero over most of the machine.

If ϵ for all the particles were the same, the cloud of points would rotate unchanged with angular velocity constant. Since however there is a spread in r.f. phase, the different particles have different values of ϵ . Angular stretching of the cloud occurs, until ultimately it has an annular shape. The coherent oscillations have become converted into incoherent oscillations, as indicated in fig. 2.

First Harmonic Imperfections

It is important to consider the effect on the particle motion of first harmonic terms in the angular dependence of B. These can occur as imperfections in the magnet, but they are also deliberately inserted to correct for ion source misalignment or to aid extraction. The normalized harmonic amplitude, h , is typically of order a few parts in 10^4 . Because of the finite number of turns in the machine both $Q - 1$ and h can vary significantly in $1/(Q - 1)$ turns, especially near the centre. The concept of a resonance is no longer sharp, since a particle must make $1/\Delta Q$ turns to distinguish between Q and $Q + \Delta Q$. Familiar concepts such as free and forced oscillations are of limited use; when $Q - 1$ is small it is more convenient to use a graphical method, in which the effect of harmonics on a particle represented by a point in fig. 1 is followed turn by turn. We note first that when $Q - 1$ is small there will be, in addition to the precession, a vector change in \vec{A} equal to $\vec{\omega} \tau$ in a direction perpendicular to the direction in which the maximum of the harmonic lies. If harmonics are present, the points in fig. 2 no longer move in circles, but A changes. If there is no precession \vec{A} changes linearly, and the situation is resonant. As before ϵ is different for different particles, and in general A_x and A_y increase. Harmonic coil correction of ion source offset consists of adjusting h to such a value that $A_x = 0$ for values of r sufficiently great that $h = 0$.

The locus of A is given by

$$\begin{aligned}\Delta A_x &= -\pi h_y \tau - 2\pi(1-Q)A_y \\ \Delta A_y &= \pi h_x \tau + 2\pi(1-Q)A_x.\end{aligned}$$

This equation is illustrated graphically in fig. 3. A_x or A_y may be eliminated to give a second order difference equation, which reduces to the standard result in the limit of small changes and $Q - 1$ small.

In the above discussion we have examined the applicability of conventional concepts of "betatron" oscillations to the isochronous cyclotron when $Q - 1$ is small. These are seen to be useful provided that we are prepared to accept a resolution equal to the turn separation. For finer detail than this, especially near the centre, a more exact (and necessarily more complicated and less general) description is required. Vertical motion presents little complication, coherent oscillations are only present in an imperfect machine, and Q is normally small so that precession is not meaningful. The distribution of amplitudes depends strongly on the central

conditions, especially the r.f. phase at which the particle leaves the source.²

Other concepts necessary for diagnosis, such as r.f. "phase slip" are straightforward and will not be discussed.

Emphasis will be on the internal beam, where the basic problem is to produce a good quality beam with suitable coherent oscillation structure at the extraction radius.

Probe techniques used in the V.E.C.

The V.E.C. has been described elsewhere³ but for convenience the leading parameters and a list of beams obtained to date are given in the appendix. It is provided with three probe positions; since these are $2\pi/3$ apart and the orbit modulation affects them equally, it may be included if desired as a correction which is a function of radius.

The most direct measurement which we use is current versus radius on a single probe. Used in conjunction with a controlled shift in frequency or magnetic field, loss due to phase slip can be located and corrected by the method of Garren and Smith.⁴ We have found this method quick and effective both for setting up and measuring r.f. phase width, which is typically 50° . Although an r.f. induction probe was provided, it has not been used. When the machine is correctly set up there is very little loss of beam with radius. With H_2^+ and heavy ions however there is a measurable loss due to stripping and charge exchange. For ϵ constant, and $\sigma \propto \gamma - 1$ the beam decreases exponentially with radius. For 5 MeV H_2^+ we found excellent agreement with the theory of Berkner et al.⁵ Another apparent loss found with protons was manifest as a sharp 2:1 "step" at 10" radius. This turned out to be due to H_3^+ ions accelerated on third harmonic, which lost synchronism at this radius.⁶

To obtain information on the coherent and incoherent radial oscillations we have used both differential probes and the shadow technique described and analysed by Garren and Smith.⁴ They assume a uniform distribution with radius of equilibrium orbit radii, with turn separation ΔR and $Q - 1$ both small. The oscillation amplitude is A , and an important parameter is $A_0 = \Delta R / 2\pi(Q - 1)$. The physical significance of A_0 is that when A/A_0 exceeds unity the orbit crosses itself, as may be seen in fig. 4. From straightforward though rather lengthy geometrical arguments they construct a set of curves showing the radius at which a moving probe will intercept a particle which would otherwise strike the fixed probe, as a function of oscillation amplitude A and phase ψ .

In fig. 5 these curves, labelled in terms of the probe separation $\Delta R/A_0$ are replotted on an $A-\psi$ plot. If the beam is represented by an assembly of points, S , then a count of points on

either side of a particular curve gives the ratio of currents to the two probes at the corresponding separation. The points in S represent in this case not a range of equilibrium orbits ΔR , but rather a range of equilibrium orbits such that the maxima of the radial oscillations lie in the range between R_u and $R_u - \Delta R$, where R_u is the radius of the upstream probe. For a distribution such that $A_i \neq 0$ it is evident that the shape and total width of the shadow will vary as S precesses. In particular, if S crosses the line X where the curves merge, steps will appear in the shadows. These have been observed in a badly adjusted machine.

This modulation of shadow shape may be seen in fig. 6 which shows shadows measured at 1" intervals. Some indication of A_c and ψ may be found from the modulation of spacing; ΔR_p , the value of ΔR when the current is equally shared by both probes, is plotted in fig. 6. (The fact that the average value of ΔR_p should be zero may be used to check the probe calibration.) The reason for the sudden disappearance of structure at 15 inches in fig. 6 is not understood.

When A_c is zero an estimate of A_i may be made from the shadow curves. As is shown by Smith and Garren (and may be seen in fig. 5), A_i is of order 1/3 the shadow width provided that $A_c > A$. For $A_c < A$ it is greater, and shadows are deceptively sharp.

Some shadows of a well centred beam, in which A_c is about 0.15 inches, are shown in fig. 7. The factors which determine A_i are complicated; we have not analysed them in detail. The values achieved to date both on fundamental and 3rd harmonic acceleration have enabled extraction efficiencies of greater than 50% to be obtained, (with the aid of a suitable A_c introduced at large radii by means of the valley coils.)

In this analysis a distribution of equilibrium orbit density which is uniform over a distance greater than the turn spacing is assumed; shadow methods are less appropriate when turn separation exists. To examine turn separation a differential probe which measures current density as used by Steimel for example⁷ is preferable. Coherent oscillations can then be seen directly as a modulation of turn spacing. In our machine, where r.f. phase selection at the centre is not attempted, the turn structure cannot in general be resolved; nevertheless we have found a differential probe useful for giving a quick idea of beam quality. We have not attempted detailed analysis of such plots, but we know that a "spiky" plot denotes large coherent oscillations. Attempts to calculate how to move the ion source to remove these oscillations by analysing the position and size of the spikes has not been very successful, and we find that systematic trial and error methods are more satisfactory. A differential plot corresponding to the shadows in fig. 7 is shown.

To illustrate the form of differential probe curves a simple idealized situation will be studied.

Consider a system which initially has uniform turn spacing and no oscillations. Suppose now that some perturbation is introduced (e.g by moving the source) such that an oscillation is introduced of amplitude A with maximum in direction ψ at $\theta = \theta_0$. Then $dr/d\theta$ consists of two parts, one due to orbit spiralling and one due to precession. It is easy to show that the current on the probe is given by⁶

$$i \propto r / [\epsilon r_0^2 + 2\pi A r (1-Q) \sin\{2\pi/\epsilon r_0\} (1-Q) dB - \psi_0^2].$$

If $A = 0$, i increases uniformly with r . For A small, the curve is modulated at the precession frequency; as A increases the maxima become more spiky, becoming infinite at a radius such that $|2\pi(1-Q)| \approx \epsilon r_0^2 / Ar = \Delta R/A$. This is just the "crossing" criterion of fig. 4. At even larger values of A the second term in the denominator becomes negative, the peak "splits" and the simple formula equation 5 is then no longer applicable to the region between the peaks (c.f klystron bunching theory, where a similar phenomenon occurs when overtaking sets in.)

From the position of the peaks, ψ may be determined, and from the ratio S of a maximum to its adjacent minimum A may be found from the relation

$$S = \frac{1 + 2\pi A r (1-Q) / \epsilon r_0^2}{1 - 2\pi A r (1-Q) / \epsilon r_0^2} \quad (5)$$

Such a curve with parameters appropriate to the V.E.C. is shown in fig. 8. Agreement with measured curves however is poor; one of the difficulties is that because of scalloping and beam penetration the geometry of the probe is not easy to define. Some measured curves corresponding to a low energy setting showing both "spikes" and turn separation are given in fig. 9.

Measurements of vertical oscillation amplitude have been made using conventional three finger probes; the beam is typically 1/8 - 1/4" in vertical extent at entry to the deflector. It is well centred. The $Q_R = 2 Q_V$ coupling resonance has been observed, and extraction achieved both with the deflector before and after the resonance.

Extracted Beam

Numerous measurements have been made on the position, emittance and energy spread of various external beams. Methods used and results obtained are comparable with those of other cyclotrons of this type. At the time of writing the topic of particular interest is heavy ion extraction, both with third harmonic and fundamental operation. Extraction efficiency is typically 40-60%, and a list of beams so far extracted is given in the appendix.

Acknowledgements

The work described has been done by various members of the cyclotron team. More details of the internal beam studies are given by Bennett et al⁶; as yet, accounts of the external beam work are

contained only in unpublished internal notes.

References

1. J.D. Lawson, Nucl.Inst. and Meth. to be published 1967.
2. P. Kramer et al, CERN 63-19 (Geneva Conference) 1963, p. 214.
3. J. D. Lawson, Rutherford Laboratory Report NIRL/R/85, 1965.
4. A. A. Garren and Lloyd Smith, CERN 63-19 (Geneva Conference) 1963, p. 18.
5. K. H. Berkner et al, Phys. Rev. 160, 1961, p. 9.
6. J. R. J. Bennett et al, Rutherford Laboratory Report RHEL/R 135, 1966.
7. H. Steimel, CERN 63-19 (Geneva Conference) 1963, p. 24.
8. H. A. Grunder and F. B. Selph, CERN 63-19 (Geneva Conference) 1963 p. 8.

Appendix

Parameters of the Harwell Variable Energy Cyclotron

Energy: Up to 50 MeV for protons, $80 N^2/A$ for other ions.

Magnet: 70 inch pole diameter, 3 spiral ridges, $7\frac{1}{2}$ " minimum gap.

R.F. 1 180° dee, 1.6 inch aperture; up to 100 kV peak voltage fed by 240 kW transmitter. Dee tuned by resonant line with movable short.

Extractor: Two electrostatic channels (48° and 56°) with adjustable gap and positioning. The second channel is curved in the vertical direction to provide radial focusing.

Ion Source: Standard hooded arc, variable in position and orientation.

Energies (MeV) of extracted beams: (* denotes beam supplied for users):

H^+ : 13*, 20*, 27*, 53*	H_2^+ : 5, 27*, 42
He^+ : 8*	He^{++} : 40*, 53*, 84
C^{3+} : 24	O^{4+} : 32
	Ne^{3+} : 36

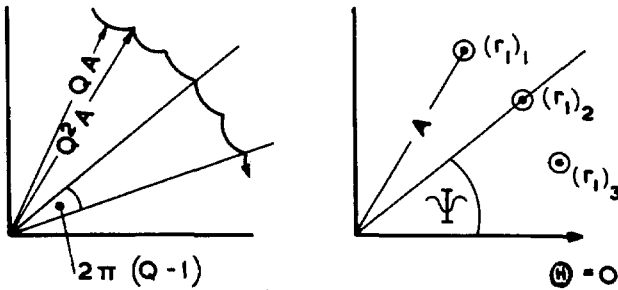


Fig. 1. Representation of particle orbit in terms of (a) the locus of the centre of curvature of the orbit or (b) (more conveniently) the amplitude and direction of the maximum of the radial oscillation ($A - \Psi$ plot).

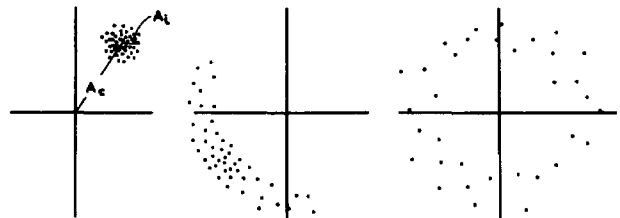


Fig. 2. Distribution of values of A and Ψ for a group of particles showing growth of A_1 as r increases. (A suitable convention, e.g. equilibrium orbits in a band of radii Δr , must be chosen so that each particle is only counted once.)

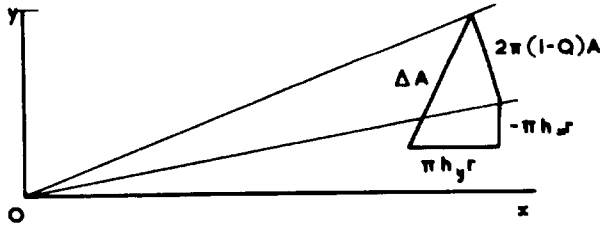


Fig. 3. Graphical representation of equation 3.

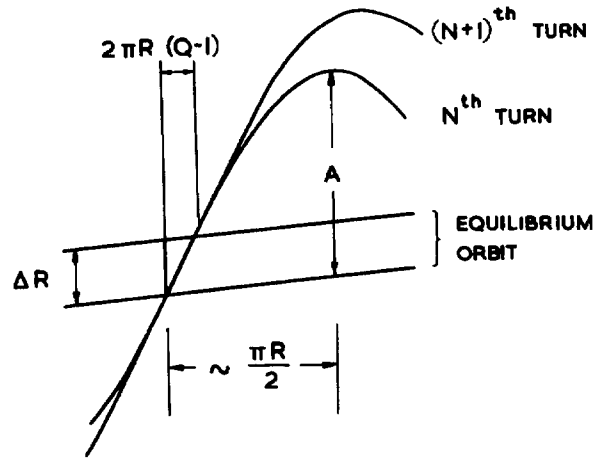


Fig. 4. Criterion for orbit to touch itself on successive revolutions, $A = \Delta R / 2\pi(Q - 1) = A_0$.

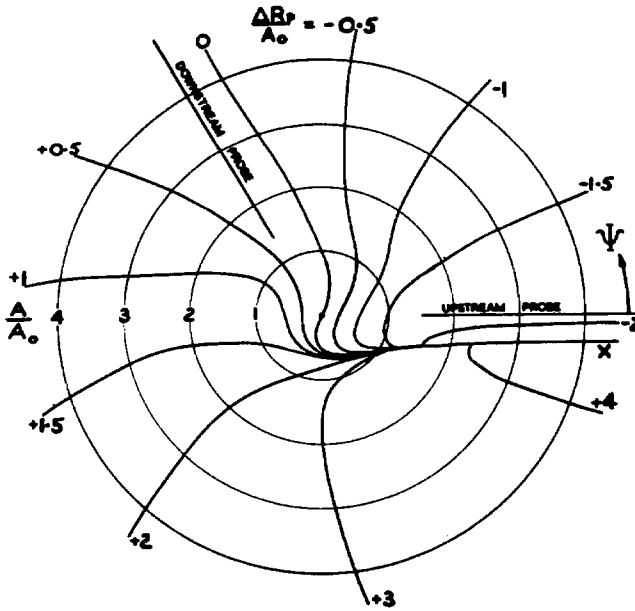


Fig. 5. Chart to show which of two probes spaced 120° apart a particle with given A, Ψ will strike. ΔR_p is the difference in radii of downstream and upstream probes. Particles with A, Ψ on the same side of a ΔR_p curve as the $\Psi = 0$ axis will strike the upstream or downstream probe according as $Q >$ or < 1 . (This curve is Fig. 7 of ref. 4 replotted.) The convention for specifying on which turn a point should be plotted is discussed in the text.

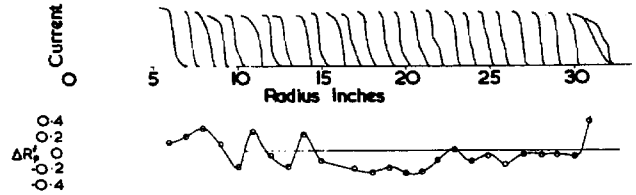


Fig. 6. Measured shadow curves and a plot of $\Delta R_p/A_0$, the value of ΔR_p when the current on both probes is equal, for a poorly centred 50 MeV proton beam.

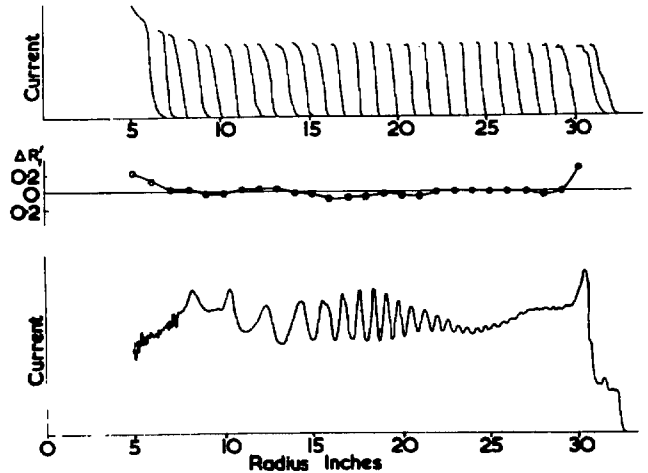


Fig. 7. Similar curves for a well centred beam, together with a differential probe plot.

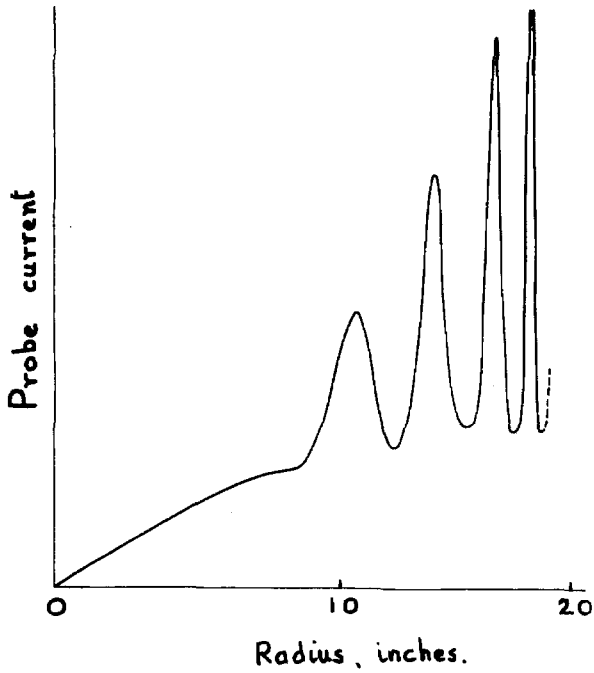


Fig. 8. Theoretical idealized differential probe plot calculated from equation 5 with $A = 0.2''$, using values of Q and ϵ appropriate to 50 MeV protons accelerated with a dee voltage of 50 kV in the V.E.C.

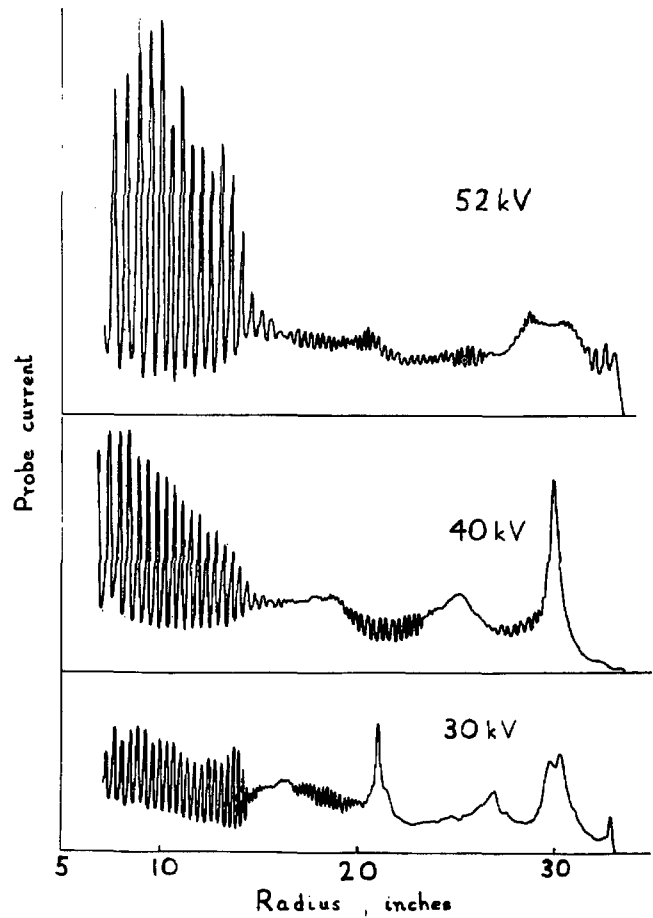


Fig. 9. Actual differential probe plots for 8 MeV He⁺ accelerated on third harmonic. Individual turn structure as well as peaks of the type illustrated by fig. 8 may be seen.